

## Do Stops Slow Down Electroweak Bubble Walls?

P. John<sup>1</sup> and M.G. Schmidt<sup>2</sup>

*Institut für Theoretische Physik, Philosophenweg 16, D-69120 Heidelberg,  
Germany*

### Abstract

We compute the wall velocity in the MSSM. We therefore generalize the SM equations of motion for bubble walls moving through a hot plasma at the electroweak phase transition and calculate the friction terms which describe the viscosity of the plasma. We give the general expressions and apply them to a simple model where stops, tops and W bosons contribute to the friction. In a wide range of parameters including those which fulfil the requirements of baryogenesis we find a wall velocity of order  $v_w \approx 10^{-2}$  much below the SM value.

*PACS:* 12.60.Jv; 11.10Wx; 98.80.Cq; 11.15.Kc

*Keywords:* Supersymmetry; Electroweak phase transition; Bubble wall velocity

---

<sup>1</sup>P.John@thphys.uni-heidelberg.de

<sup>2</sup>M.G.Schmidt@thphys.uni-heidelberg.de

# 1 Introduction

The generation of the baryon asymmetry of the Universe in a first order phase transition (PT) of the electroweak theory is attractive because all of its ingredients could be tested in high energy experiments in the near future. However, it is for sure now that there is no strong first order PT in the Standard Model (SM) with a Higgs mass above the experimental lower bound, indeed there is no PT at all [1]. The SM is very successful, but there is common agreement that it has to be extended to a more general theory. That this theory will contain supersymmetry is still controversial but in lack of alternatives this is a very useful hypothesis. In the MSSM and also in an extension with an additional singlet field (NMSSM) [2–4] it is possible to obtain a strong first order PT without violating the experimental Higgs mass bounds. In the MSSM this is related to a scalar partner of the right handed top which is very light in the symmetric phase [5–7]. It increases the cubic term in the effective 1-loop scalar potential. In the NMSSM a  $SH_1H_2$  term arises already at tree level and acts effectively as a  $\phi^3$ -term if the vacuum expectation value (vev)  $\langle S \rangle$  is comparable to the Higgs vevs [8]. These types of models have also more freedom to realize CP-violating effects. It is well known that supersymmetric models allow for spontaneous CP-violation at  $T = 0$ . The parameter space is strongly restricted by experimental bounds on the electric dipole moment of the neutron (for a discussion and references see e.g. [9]). Moreover to produce a baryon asymmetry at the electroweak scale CP-violation within the bubble wall is needed. Therefore it has been proposed that a temperature induced transitional CP-violation might occur [10–12]. In [13,14] it was shown that in the MSSM spontaneous CP-violation does not occur throughout. Even with maximal explicit CP violating phases the variation of the corresponding phase in the Higgs system is strongly suppressed.

The baryon asymmetry arises in a two step process: first the expanding wall sweeps through the hot plasma separating Higgs phase and symmetric phase with a CP-violating spatially varying Higgs vev. It generates an asymmetry between left handed quarks and their antiparticles diffusing in front of the bubble starting from an asymmetry between stops, tops, charginos, neutralinos and their antiparticles. In a second step this asymmetry in the hot plasma in front of the bubble wall is transformed into a baryon asymmetry through (hot) unsuppressed sphaleron transitions. If the PT is strongly first order this asymmetry is not destroyed by the Higgs phase (weak) sphaleron when finally the equilibrium phase

takes over. The rise of the generated baryon asymmetry depends on the spatial variation of the CP-violating phase in the wall. Moreover, in the MSSM the variation  $\Delta\beta \sim d\beta/dx$  of  $\tan\beta$  is an important ingredient for the determination of the baryon asymmetry  $\eta$ . Due to its smallness the observed baryon asymmetry may be reached only in a small, eventually tuned range [15] of parameters and therefore also a better knowledge of the wall velocity is needed, since there is a strong dependency on it. For instance in [16] it was found in semiclassical calculations that with a given Higgs field profile  $h^2(x)$

$$\eta \sim \int_{-\infty}^{\infty} dx \frac{h^2(x)}{v_w T_c^2} \frac{d\beta(x)}{dx}. \quad (1.1)$$

Thus the asymmetry increases with decreasing wall velocity. Of course  $v_w \rightarrow 0$  is not possible, in this case there would be no out-of-equilibrium region. Quite naively one might expect that more particles would imply more interactions and in consequence a higher viscosity of the plasma. For this reason it usually was assumed (e.g. [17]) that the velocity of bubble walls of supersymmetric phase transitions is smaller than the velocity in the SM. But that has to be shown in a detailed calculation.

To go beyond speculations we want to reconsider this question and the calculation of the wall velocity taking into account also supersymmetric particles. The proceeding is similar to that of [18]. Nevertheless, in case of two (Higgs-) scalars and arbitrarily many interacting particle species (fermions *and* bosons), the calculation and the results differ considerably from [18]. Therefore, we will explicitly outline the main steps of the calculation (see also [13]) to demonstrate the differences. On the other hand, at some points which can be found in [18] we keep short in the representation.

## 2 Bubble Wall Equation of Motion

Energy conservation leads to the equations of motion of an electroweak bubble wall interacting with a hot plasma of particles [18–20]:

$$\square h + V'(h) + \sum_i \frac{\partial m_i^2}{\partial h} \int \frac{d^3k}{(2\pi)^3 2E} f_i(k, x) = 0, \quad (2.1)$$

where  $f_i = f_{0,i} + \delta f_i$  is the distribution function for a particle species in the heat bath. We have to sum over all particle species  $i$ . The distribution function is

divided up into equilibrium part  $f_{0,i}$  and out-of-equilibrium part  $\delta f_i$ . For two scalars (or more, analogously) we obtain

$$\square h_1 + \frac{\partial V_T(h_1, h_2)}{\partial h_1} + \sum_i \frac{\partial m_i^2}{\partial h_1} \int \frac{d^3 p}{(2\pi)^3 2E_i} \delta f_i(p, x) = 0, \quad (2.2)$$

$$\square h_2 + \frac{\partial V_T(h_1, h_2)}{\partial h_2} + \sum_j \frac{\partial m_j^2}{\partial h_2} \int \frac{d^3 p}{(2\pi)^3 2E_j} \delta f_j(p, x) = 0. \quad (2.3)$$

The equilibrium part has been absorbed into the equilibrium temperature dependent effective potential  $V_T(h_1, h_2)$ . In equilibrium we would obtain the free equations for critical bubbles respectively domain walls for large radii.

In the following we will restrict ourselves to late times leading to a stationarily moving domain wall where the friction stops the bubble wall acceleration. This is the long period of bubble expansion where baryogenesis takes place. The influence of different friction or viscosity terms in Standard type models was investigated in various papers [19–21]. We assume not too large velocities and check the self consistency of this assumption in the MSSM.

### 3 Fluid Equations

Now we want to derive the deviations  $\delta f_i$  from the equilibrium population densities originating from a moving wall. We will therefore discuss the Boltzmann equation in the fluid frame, the "fluid equations":

$$d_t f_i \equiv \partial_t f_i + \dot{x} \frac{\partial}{\partial x} f_i + \dot{p}_x \frac{\partial}{\partial p_x} f_i = -C[f_i], \quad (3.1)$$

with the population density  $f_i$  and energy  $E = \sqrt{p_x^2 + m^2(x)}$ .  $C[f_i]$  represents the scattering integral and will be discussed in section 6. The classical (WKB) approximation is valid for

$$p \gg \frac{1}{L_w} \quad (\text{"thick wall"}). \quad (3.2)$$

For particles with  $E, p \gtrsim gT$  this should be fulfilled. Thus, here infrared particles are supposed not to contribute to the friction [18–20]. This is a crude approximation. A further understanding of the infrared particle contribution is therefore needed which goes beyond the aim of this paper<sup>3</sup>. In the MSSM the wall thickness  $L_w$  is of order  $15/T$ – $40/T$ , as found in [7, 13, 22], and  $L_w \gg 1/T$  is fulfilled.

---

<sup>3</sup>Ref. [28] revisits the calculation of the friction in the SM. The prediction is that hard thermal loop effects play an important role in the damping of the gauge fields in the hot phase and that such coherent gauge field contributions are very effective for generating a friction.

With [18] we denote those particles which couple very weakly to the Higgs as “light particles”. Particles coupling strongly to the Higgs are heavy in the Higgs phase and therefore called “heavy”. However, “superheavy” particles as the “left handed” stops do not appear in our calculation besides their remnants in the effective potential. We treat as “heavy” particles only top quarks, (right handed) stops, and W bosons. Besides for the physical stop mass, we neglect the  $U(1)$  and treat only the  $SU(2)$  with its coupling  $g$ . The Higgses are left out.

We assume now that the interaction between wall and particle plasma is the origin of small perturbations from equilibrium. We will treat perturbations in the temperature  $\delta T$ , velocity  $\delta v$  and chemical potential  $\delta\mu$  and linearize the resulting fluid equations. Then the full population density  $f_i$  of a particle species  $i$  in the fluid frame is given by

$$f_i = \frac{1}{\exp\left\{\frac{(E+\delta_i)}{T}\right\} \pm 1}, \quad (3.3)$$

where we have generally space dependent perturbations  $\delta_i$  from equilibrium. In principle one must include perturbations from the global value for each particle species. A simplification is to treat all the “light” particle species as one common background fluid. This background fluid obtains common perturbations  $\delta v_{bg}$  in the velocity and  $\delta T_{bg}$  in the temperature. This leads us to

$$\delta_i = - \left[ \delta\mu_i + \frac{E}{T}(\delta T_i + \delta T_{bg}) + p_x(\delta v_i + \delta v_{bg}) \right] \quad (3.4)$$

for the “heavy” particles. The spatial profiles of all these perturbations depend on the microscopic physics. We treat particles and antiparticles as one species neglecting CP violation which is a minor effect on the friction. For the calculation of the baryon asymmetry this is the important effect and would be involved in eq. (3.4) by a perturbation  $\delta E_{\pm}$  in the energy dividing particles and antiparticles [4, 23].

We now expand  $d_t f$  to linear order in the perturbations. The Boltzmann equation can then be written as

$$\begin{aligned} & (-f'_0) \left( \frac{p_x}{E} [\partial_x \delta\mu + \frac{E}{T} \partial_x (\delta T + \delta T_{bg}) + p_x \partial_x (\delta v + \delta v_{bg})] + \partial_t \delta\mu \right. \\ & \left. + \frac{E}{T} \partial_t (\delta T + \delta T_{bg}) + p_x \partial_t (\delta v + \delta v_{bg}) \right) + TC(\delta\mu, \delta T, \delta v) = (-f'_0) \frac{\partial_t(m^2)}{2E}. \end{aligned} \quad (3.5)$$

The term on the right hand side of (3.5) drives the population density away from equilibrium.

The collision term depends on all perturbations. But since the perturbations are Lagrangian multipliers for particle number, energy, and momentum, we can determine the parameters by the appropriate integration choice

$$\int \frac{d^3p}{(2\pi)^3}, \quad \int E \frac{d^3p}{(2\pi)^3}, \quad \text{and} \quad \int p_x \frac{d^3p}{(2\pi)^3}. \quad (3.6)$$

The resulting three equations coming from the Boltzmann equation, the ‘‘fluid equations’’, are coupled through the collision term  $C[\delta\mu, \delta T, \delta v]$ . Performing the integrals leads to the general pattern

$$\begin{aligned} \int \frac{d^3p}{(2\pi)^3 T^2} C[f] &= \delta\mu \Gamma_{\mu_1} + \delta T \Gamma_{T_1}, \\ \int \frac{d^3p}{(2\pi)^3 T^3} E C[f] &= \delta\mu \Gamma_{\mu_2} + \delta T \Gamma_{T_2}, \\ \int \frac{d^3p}{(2\pi)^3 T^3} p_x C[f] &= \delta v \Gamma_v, \end{aligned} \quad (3.7)$$

where the rates  $\Gamma$  are of the form  $\Gamma \sim \alpha^2 \ln(1/\alpha)T$ , and  $\alpha = g^2/(4\pi)$  is the gauge coupling.

The expressions (3.7) have to be evaluated graph by graph through the out of equilibrium interactions of each particle species. In sec. 6 we will calculate the leading contributions.

For a stationary wall we can use  $\partial_t \delta_i \rightarrow v_w \delta'_i$ , and  $\partial_z \delta_i \rightarrow \delta'_i$ , where the prime denotes the derivative with respect to  $z = x - v_w t$  (Galilei transformation for small  $v_w$ ).

In the following the equations are again similar to those in [18] but there are important additional terms. We can solve the fluid equations to eliminate the background perturbations  $\delta v'_{bg}$  and  $\delta T'_{bg}$ :

$$\delta T'_{bg} = \frac{-v_w(A+B) + C + D}{\bar{c}_4(\frac{1}{3} - v_w^2)}, \quad (3.8)$$

$$\delta v'_{bg} = \frac{A + B - 3v_w(C + D)}{T\bar{c}_4(\frac{1}{3} - v_w^2)}, \quad (3.9)$$

where we have used the notation

$$\begin{aligned}
A &= \sum_{\text{fermions } f} N_f(\delta\mu_f\Gamma_{\mu 2f} + \delta T_f\Gamma_{T 2f}), \\
B &= \sum_{\text{bosons } b} N_b(\delta\mu_b\Gamma_{\mu 2b} + \delta T_b\Gamma_{T 2b}), \\
C &= \sum_{\text{fermions } f} N_f\delta v_f T\Gamma_{vf}, \\
D &= \sum_{\text{bosons } b} N_b\delta v_b T\Gamma_{vb}.
\end{aligned} \tag{3.10}$$

In contrast to the computations in [18] these terms may include arbitrarily many fermions and bosons, respectively.

We can see that for walls moving with the velocity of sound  $v_w = v_s = 1/\sqrt{3} \approx 0.577$ , the approximation obviously breaks down. This demonstrates the limit of the expansion in linear perturbations.

For each heavy particle species in the plasma we have three fluid equations resulting from the combination of eqs. (3.5), (3.6) and (3.7). The final form of the fluid equations can be written in a matrix notation:

$$\mathbb{A}\delta' + \Gamma\delta = F, \tag{3.11}$$

where

$$\Gamma = \Gamma_0 + \frac{1}{\bar{c}_4}\mathbb{M}. \tag{3.12}$$

The matrices  $\mathbb{A}$ ,  $\Gamma$ ,  $\Gamma_0$ , and  $\mathbb{M}$  are given below. The number  $\bar{c}_4$  is the heat capacity of the plasma  $\bar{c}_4 = 78c_{4-} + 37c_{4+}$  including light quarks, leptons, and sleptons in the plasma. The number changes when we include further light particles. The perturbations are combined in a vector  $\delta$ , the driving terms are combined in the vector  $F$ . The driving term containing  $(m^2)'$  can be split up into different contributions

$$(m^2)' = \frac{\partial m^2}{\partial h_1}h_1' + \frac{\partial m^2}{\partial h_2}h_2'. \tag{3.13}$$

The vector  $\delta$  and the matrices for  $k$  particle species (index  $x$  denotes + or -, for fermions and bosons, respectively, for the  $i$ th particle):

$$\delta = [\delta\mu_1 \quad \delta T_1 \quad T\delta v_1 \quad \dots \quad \delta\mu_k \quad \delta T_k \quad T\delta v_k]^T, \tag{3.14}$$

$$F = \frac{v_w}{2T} [c_{1x}(m_1^2)' \quad c_{2x}(m_1^2)' \quad 0 \quad \dots \quad c_{1x}(m_k^2)' \quad c_{2x}(m_k^2)' \quad 0]^T. \tag{3.15}$$

The matrices  $\mathbb{A}$  and  $\Gamma$  are of block diagonal form:

$$\mathbb{A} = \begin{bmatrix} \mathbb{A}_1 & & \\ & \ddots & \\ & & \mathbb{A}_k \end{bmatrix}, \quad \text{where} \quad \mathbb{A}_i = \begin{bmatrix} v_w c_{2i} & v_w c_{3i} & \frac{c_{3i}}{3} \\ v_w c_{3i} & v_w c_{4i} & \frac{c_{4i}}{3} \\ \frac{c_{3i}}{3} & \frac{c_{4i}}{3} & \frac{v_w c_{4i}}{3} \end{bmatrix}, \quad (3.16)$$

$$\Gamma_0 = \begin{bmatrix} \Gamma_1 & & \\ & \ddots & \\ & & \Gamma_k \end{bmatrix}, \quad \text{where} \quad \Gamma_i = \begin{bmatrix} \Gamma_{\mu 1,i} & \Gamma_{\mu 2,i} & 0 \\ \Gamma_{T 1,i} & \Gamma_{T 2,i} & 0 \\ 0 & 0 & \Gamma_{v,i} \end{bmatrix}. \quad (3.17)$$

Moreover,  $\mathbb{M}$  is a square matrix of the form

$$\mathbb{M} = \begin{bmatrix} M_{1,1} & \cdots & M_{1,k} \\ \vdots & \ddots & \vdots \\ M_{k,1} & \cdots & M_{k,k} \end{bmatrix}, \quad (3.18)$$

$$M_{i,j} = N_i \begin{bmatrix} c_{3i} \Gamma_{\mu 2,j} & c_{3i} \Gamma_{T 2,j} & c_{3i} \Gamma_{v,j} \\ c_{4i} \Gamma_{\mu 2,j} & c_{4i} \Gamma_{T 2,j} & c_{4i} \Gamma_{v,j} \\ c_{4i} \Gamma_{\mu 2,j} & c_{4i} \Gamma_{T 2,j} & c_{4i} \Gamma_{v,j} \end{bmatrix}, \quad i, j = 1 \dots k, \quad (3.19)$$

where  $i$  in  $c_{3i}$ ,  $c_{4i}$  denotes fermionic or bosonic contributions  $c_{3\pm}$ ,  $c_{4\pm}$  of the  $i$ th and  $j$ th particle species, respectively. They are defined for fermions(+) and bosons(-) through

$$c_{n\pm} = \int \frac{E^{n-2}}{T^{n+1}} f'_0(\pm) \frac{d^3 p}{(2\pi)^3}. \quad (3.20)$$

## 4 Higgs Equation of Motion and Friction

With the definition (3.20) and taking into account (righthanded) stop-, top- and  $W$  particles the equations of motion can be approximated in the fluid picture as

$$\begin{aligned} 0 &= -h_1'' + \frac{\partial V_T}{\partial h_1}(h_1, h_2) + \frac{N_W}{2} T \frac{dm_W^2}{dh_1} (c_{1-} \delta\mu_b + c_{2-} \delta T_W + c_{2-} T \delta v_W), \\ 0 &= -h_2'' + \frac{\partial V_T}{\partial h_2}(h_1, h_2) + \frac{N_W}{2} T \frac{dm_W^2}{dh_2} (c_{1-} \delta\mu_W + c_{2-} \delta T_W + c_{2-} T \delta v_W) \\ &+ \frac{N_t}{2} T \frac{dm_t^2}{dh_2} (c_{1+} \delta\mu_t + c_{2+} \delta T_t + c_{2+} T \delta v_t) \\ &+ \frac{N_{\tilde{t}_1}}{2} T \frac{dm_{\tilde{t}_1}^2}{dh_2} (c_{1-} \delta\mu_{\tilde{t}} + c_{2-} \delta T_{\tilde{t}} + c_{2-} T \delta v_{\tilde{t}}). \end{aligned} \quad (4.1)$$

This can formally be rewritten as

$$\begin{aligned}
-h_1'' + \frac{\partial V_T}{\partial h_1}(h_1, h_2, T) + \frac{T}{2}h_1G_1\delta_1 &= 0, \\
-h_2'' + \frac{\partial V_T}{\partial h_2}(h_1, h_2, T) + \frac{T}{2}h_2G_2\delta_2 &= 0,
\end{aligned} \tag{4.2}$$

with

$$G_1 = \begin{bmatrix} N_W c_{1-} g^2/2 \\ N_W c_{2-} g^2/2 \\ N_W c_{2-} g^2/2 \\ 0 \\ 0 \\ 0 \\ 0 \\ 0 \\ 0 \end{bmatrix}, \quad G_2 = \begin{bmatrix} N_W c_{1-} g^2/2 \\ N_W c_{2-} g^2/2 \\ N_W c_{2-} g^2/2 \\ N_{\bar{t}} c_{1-} y_{\bar{t}}^2 \\ N_{\bar{t}} c_{2-} y_{\bar{t}}^2 \\ N_{\bar{t}} c_{2-} y_{\bar{t}}^2 \\ N_t c_{1+} y_t^2 \\ N_t c_{2+} y_t^2 \\ N_t c_{2+} y_t^2 \end{bmatrix}, \quad \delta_1 = \begin{bmatrix} \delta\mu_W \\ \delta T_W \\ T\delta v_W \\ \delta\mu_{\bar{t}} \\ \delta T_{\bar{t}} \\ T\delta v_{\bar{t}} \\ \delta\mu_t \\ \delta T_t \\ T\delta v_t \end{bmatrix}, \quad \text{and } \delta_2 = \begin{bmatrix} \delta\mu_W \\ \delta T_W \\ T\delta v_W \\ 0 \\ 0 \\ 0 \\ 0 \\ 0 \\ 0 \end{bmatrix}. \tag{4.3}$$

The vectors  $\delta_1, \delta_2$  in eq. (4.3) contain the perturbation functions which can be found as solution of eq. (3.11). Here we used the splitting of the perturbation vector we discussed at eq. (3.13). Thus one is lead to a system of linear, coupled differential equations. It can be solved numerically. The solutions give the profiles of the perturbations in the wall. Such profiles are discussed in [21] for single scalar models. We now use again the thick wall limit. First we now approximate  $\delta' = 0$ . (This will be improved later on). Then we can solve eq. (3.11) for the perturbation vectors  $\delta_{1,2}$ :

$$\delta_{1,2} = \Gamma^{-1} F_{1,2}. \tag{4.4}$$

We obtain  $F_{1,2}$  for stops, top and  $W$  from eq. (3.11) in the simplified form

$$F_2 = \frac{v_w}{2T} \begin{bmatrix} c_{1-} (m_W^2)' \\ c_{2-} (m_W^2)' \\ 0 \\ c_{1-} (m_{\bar{t}}^2)' \\ c_{2-} (m_{\bar{t}}^2)' \\ 0 \\ c_{1+} (m_t^2)' \\ c_{2+} (m_t^2)' \\ 0 \end{bmatrix} = \frac{v_w}{2T} h_2 h_2' \begin{bmatrix} c_{1-} g^2/2 \\ c_{2-} g^2/2 \\ 0 \\ c_{1-} y_{\bar{t}}^2 \\ c_{2-} y_{\bar{t}}^2 \\ 0 \\ c_{1+} y_t^2 \\ c_{2+} y_t^2 \\ 0 \end{bmatrix} \equiv \frac{v_w}{2T} h_2 h_2' \tilde{F}_2, \tag{4.5}$$

and

$$F_1 = \frac{v_w}{2T} \begin{bmatrix} c_1 - (m_W^2)' \\ c_2 - (m_W^2)' \\ 0 \end{bmatrix} = \frac{v_w}{2T} h_1 h_1' \begin{bmatrix} c_1 - g^2/2 \\ c_2 - g^2/2 \\ 0 \end{bmatrix} \equiv \frac{v_w}{2T} h_1 h_1' \tilde{F}_1. \quad (4.6)$$

Finally, we arrive at the bubble wall equations of motion with friction,

$$\begin{aligned} h_1'' - V_T' &= \eta_1 v_w \frac{h_1^2}{T} h_1', \\ h_2'' - V_T' &= \eta_2 v_w \frac{h_2^2}{T} h_2'. \end{aligned} \quad (4.7)$$

The dimensionless constants  $\eta_1$  and  $\eta_2$  are defined through the relation

$$\eta_1 = \frac{T}{4} G_1 \Gamma^{-1} \tilde{F}_1, \quad (4.8)$$

$$\eta_2 = \frac{T}{4} G_2 \Gamma^{-1} \tilde{F}_2, \quad (4.9)$$

where we used the definitions for  $G_{1,2}$  in eq. (4.3) and  $\tilde{F}_{1,2}$  from eqs. (4.5) and (4.6) above. The factor  $T$  rescales  $\Gamma^{-1} \sim T^{-1}$ . The friction terms  $\eta_1$  and  $\eta_2$  are still slightly  $\tan\beta$ -dependent. The constants give the viscosity of the medium which is perturbed by the moving wall surface. But since  $\delta'$  in general is not negligible we need the full solution to eq. (3.11) and  $\eta_{1,2}$  cannot be defined as in eqs. (4.8) and (4.9) and the r.h.s. of (4.7) maintain an implicit  $v_w$ -dependence beside the factor. We then have to solve eq. (4.2) directly instead of eq. (4.7). In the next section we proceed with (4.7) in order to obtain an analytical formula for the wall velocity which is useful in any case.

## 5 Wall Velocity in the MSSM

In order to solve eqs. (4.7) we derive a virial theorem, based on the necessity that for a stationary wall the pressure to the wall surface is balanced by the friction: the pressure from inside the bubble which is responsible for the expansion and the pressure resulting from the viscosity of the plasma must be equal. The pressure on a free bubble wall can be obtained from l.h.s. of the equation of motion (4.7) by

$$p_1 = \int_0^\infty \left( h_1'' - \frac{\partial V_T}{\partial h_1} \right) h_1' dx = V_T(h_1(0)) - V_T(h_1(x = \infty)) = \Delta V_T, \quad (5.1)$$

which is compensated due to the friction term, the r.h.s. of (4.7):

$$\int \left( h_1'' - \frac{\partial V_T}{\partial h_1} \right) h_1' dx = \int \eta_1 v_w \frac{h_1^2}{T} (h_1')^2 = \Delta V_T, \quad (5.2)$$

where  $\Delta V_T$  is the difference in the effective potential values at the transition temperature  $T_n$ , which is basically the nucleation temperature.

Since we have two equations of the same type for each of the Higgs scalars and both of them develop friction terms, we have to add the pressure on the bubble surface. They are different due to the different particle species and couplings. Thus we find different pressures which would lead to different wall velocities, if the equations were completely decoupled. But due to the effective potential which couples the equations of motion we have back-reaction. This leads to a change in  $\Delta\beta = \max(\partial\beta/\partial z)$ . It might be interesting to investigate this question in more detail, since a larger  $\Delta\beta$  is highly welcome to obtain a larger baryon asymmetry. This point gets even more important with the knowledge of the results of [13, 14] where we realized that in the MSSM transitional CP violation does not occur. Therefore we must exploit the explicit phases which may nevertheless be strongly restricted by experimental bounds. The determination of  $\Delta\beta$  may be done numerically by solving eqs. (4.7) with extensions of the methods of [13, 24, 25].

For our estimate of the wall velocity we will use as approximation a constant  $\tan\beta$  since the deviation is so strongly suppressed as found in [7, 22, 24]. Then we can add the expressions for the pressure for both Higgs fields,  $p_1$  and  $p_2$ :

$$p_1 + p_2 = \frac{v_w}{T} \left\{ \eta_1 \int h_1^2 (h_1')^2 dx + \eta_2 \int h_2^2 (h_2')^2 dx \right\} = 2\Delta V_T. \quad (5.3)$$

Next, we define an average direction and introduce a field  $h = \sqrt{h_1^2 + h_2^2}$ . We find

$$\frac{2\Delta V_T T}{v_w} = \sin^4\beta(\eta_2 + \cot^4\beta\eta_1) \int h^2 (h')^2 dx. \quad (5.4)$$

We realize that the term corresponding to  $\eta_1$ , in comparison to the second, is strongly suppressed. Already moderately small values of  $\tan\beta=2,(3,6)$  cause roughly a suppression of order 10,(100,1000). The wall velocity is therefore predominantly determined by the second Higgs. Moreover, this behaviour also is supported by the strong Yukawa couplings of the stop and the top which couple asymmetric in favour of  $h_2$ . A ‘large’  $\tan\beta \gtrsim 2$  leads to a friction term, which

is solely determined by  $\eta_2$ . The limit  $\tan\beta \rightarrow 0$  leads to a large but finite velocity determined by the ( $\tan\beta$  dependent)  $\eta_1$ . Nevertheless, due to a different particle content  $\eta_1$  does not recover SM friction in this limit. However, the lower experimental limit is  $\tan\beta \gtrsim 2$ .

In [22, 24] it was realized that in the MSSM the approximation to the bubble wall profile by a kink is a rather good choice. Hence, we set for the common Higgs field  $h(x)$

$$h(x) = \frac{h_{crit}}{2} \left( 1 + \tanh \frac{x}{L_w} \right), \quad (5.5)$$

where  $L_w$  is the wall thickness and  $h_{crit}$  is the nontrivial vev at the nucleation temperature  $T_n$ . The integral in eq. (5.4) is evaluated as

$$\int h^2 (h')^2 dx = \frac{h_{crit}^4}{10L_w}, \quad (5.6)$$

leading to the desired equation for the wall velocity

$$v_w = \frac{20L_w}{h_{crit}^4} \frac{\Delta V_T(T_n) T_n}{\sin^4 \beta (\eta_2 + \eta_1 \cot^4 \beta)}. \quad (5.7)$$

The missing numbers for  $L_w$ ,  $h_{crit}$ ,  $T_n$ , and  $\Delta V(T_n)$  can be independently determined with methods described in [13, 22, 24, 26].

## 6 Viscosity and Wall Velocity

The next step is to determine the specific number for the friction terms. Therefore we have to calculate scattering and annihilation rates resulting from the corresponding Feynman graphs. To leading order the main contributions driving the system to equilibrium are logarithmic, coming from t-channel processes. These processes contribute to order  $g^2$ . We will drop all terms of order  $m/T$  and therefore also s-channel processes which are of order  $m^2/T^2$  (cf. [18]). The scattering amplitudes are given by the following graphs. In principle, a stop can

scatter off quarks, squarks and gluons:

$$(6.1)$$

$$(6.2)$$

In our approximation, there are only a few contributions to the matrix elements. For instance, we assume all the squarks besides the stop to be superheavy and decoupled. Hence, the first graph in (6.1) would only contribute for the stop-stop scattering. But, as the stops are at the same temperature and velocity, there is no change in the perturbations:  $\sum \delta = 0\mu + (E_p - E_{p'})\delta T + (p_z - p'_z)\delta v = 0$ . Therefore, stop-squark scattering does not contribute to the rates in this approximation.

The corresponding types of graphs have to be taken into account for the rates of the top-quark. They can scatter off gluons, quarks and squarks. Compared to the SM, a new scattering graph appears for the top which in the MSSM may scatter off squarks.

We calculate the rates which are defined in eq. (3.7) by the integration of the collision integral  $C[f]$ , hence we need

$$C[f] = \int \frac{d^3k d^3p' d^3k'}{(2\pi)^9 2E_p 2E_{p'} 2E_{k'}} |\mathcal{M}|^2 \times \\ \times (2\pi)^4 \delta(p + k - p' - k') \mathcal{P}[f]$$

with  $\mathcal{P}[f] = f_p f_k (1 - f_{p'}) (1 - f_{k'}) - f_{p'} f_{k'} (1 - f_p) (1 - f_k)$ . (6.3)

The integrals are calculated in the leading log approximation and the relativistic limit. In this approximation we find as leading contributions for the matrix elements

$$|\mathcal{M}|^2 = A_1 \cdot g_s^4 \frac{-st}{(t - m_p^2)^2}, \quad \text{and} \quad |\mathcal{M}|^2 = A_2 \cdot g_s^4 \frac{s^2}{(t - m_p^2)^2} \quad (6.4)$$

respectively where we always replace  $u \rightarrow -s$  [18]. The matrix elements give divergent rates in the limit of massless exchange particles. We therefore include thermal masses of the exchange particle  $m_p$  in the denominator. In the limit of massless outer legs we take the leading log contributions coming from the second and third graph of (6.2) only. Therefore  $m_p^2 = m_{\tilde{t}_R}^2$ . Summing over outgoing particles and averaging the incoming ones and including annihilation and scattering coming from the graphs we find  $A_1 = 1/6$  and  $A_2 = 8/3$ .

For the numerical evaluation of the resulting integrals we use  $g_s^2/(4\pi) = \alpha_s = 0.12$ ,  $\alpha_W = 1/30$ . The integrals for top-W-scattering can be found in [18]. Nevertheless, we have to reevaluate those expressions with different plasma masses for tops, W bosons, and stops since the supersymmetric plasma differs from the SM plasma [27]. We use as plasma mass of the stop for our scenario [12]

$$m_{\tilde{t}_R}^2 = -m_U^2 + \left(\frac{2}{3}g_s^2 + \frac{1}{3}h_t^2 - \frac{1}{6}(A_t^2 + \mu^2)/m_Q^2\right)T^2. \quad (6.5)$$

As a required condition for baryogenesis we need very negative  $-m_U^2$ . As plasma mass for the gluon we take  $m_g^2 \approx 2/3g_s^4T^2$ . We use  $m_W^2 = 5/6g^2T^2$  for the  $W$ -mass,  $m_t^2 = 1/6g_s^2T^2$  for the top mass. Annihilations into leptons and quarks include lepton masses  $m_l = 3/32g^2T^2$  and bosons with mass  $m_q^2 = 1/6g^2T^2$  leading to an effective plasma mass  $\ln \langle m^2 \rangle = 3/4 \ln m_q^2 + 1/4 \ln m_l^2$ .

After eliminating the perturbations with help of the rates as shown above in eqs. (3.11), (4.4) and finally eqs. (4.8) and (4.9), we can determine  $\eta_1$  and  $\eta_2$ . Numerically we find for  $\tan\beta \gtrsim \mathcal{O}(2)$  and  $m_U \lesssim \mathcal{O}(100 \text{ GeV})$

$$\eta_1 \approx \mathcal{O}(0.1), \quad (6.6)$$

$$\eta_2 \approx \mathcal{O}(100). \quad (6.7)$$

This emphasizes the domination of  $\eta_2$ . In the Standard Model with only one viscosity constant one finds roughly  $\eta_{SM} \approx 3$ . This gives rise to the hope that one will obtain the desired considerably slower walls.

The wall velocities are to be determined from the value of  $\tan\beta$  at the transition temperature  $T_n$  and the corresponding values of  $L_w$ ,  $h_{crit}$  and the difference in the potential heights  $\Delta V_T(T_n)$  from the one-loop resummed potential. In the whole scenario we assume the left handed stops to be decoupled and the right handed ones very light. We have no mixing  $A_t = \mu = 0$ ,  $m_Q = 2TeV$ , and  $m_A = 400GeV$ . For a strong PT we prefer small right handed stop parameters  $m_U^2$ . The value  $m_U^2 = -(60GeV)^2$ , thus  $m_{\tilde{t}} = 161GeV$ , is very near to the triple point [5,26]. There we find a strong phase transition with  $v/T = 0.96$  at one-loop

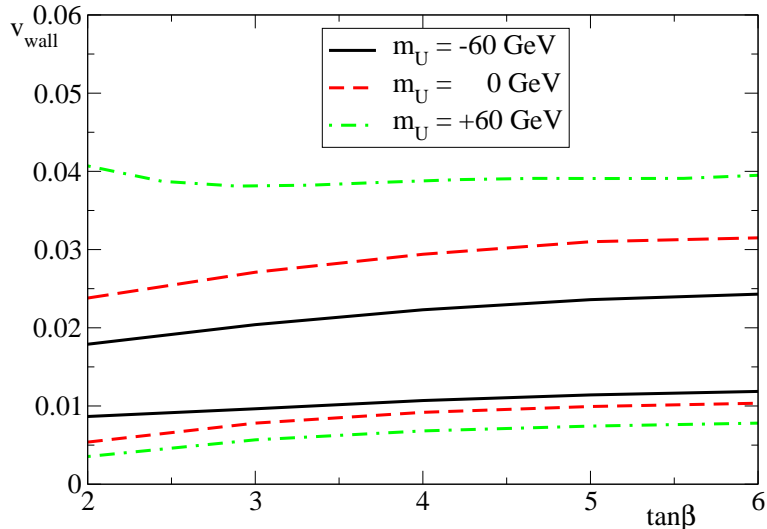


Figure 1: Wall velocity in dependence on the parameter  $\tan\beta(T=0)$  for  $m_Q = 2\text{TeV}$ ,  $A_t = \mu = 0$ , and  $m_A = 400\text{GeV}$  for  $m_U^2 = -60^2, 0, 60^2\text{GeV}^2$ . Lower bunch of graphs for  $\delta' = 0$ , upper for  $\delta' \neq 0$ .

level for  $\tan\beta = 2.0$ . At two-loop level it is even larger permitting larger  $\tan\beta$  for the same strength [5,6]. In this parameter range, eventually including some stop mixing, one can reach Higgs masses up to  $m_H \approx 110\text{ GeV}$  which agree with the present experimental bound.

In Fig. 1 the dependence on the parameter  $\tan\beta(T=0)$  is shown in the physically interesting range  $2 \leq \tan\beta \leq 6$  for three values of  $m_U^2 = -60^2, 0, 60^2\text{ GeV}^2$ . The lower bunch of curves is determined for our first approximation  $\delta' = 0$  the upper from the full numerical solution to eq. (3.11) with  $\delta' \neq 0$ . We find<sup>4</sup> corrections of roughly a factor of two for small  $m_U$  (light stop). Very heavy stops should decouple more and more which would lead to increasing wall velocities again. This behaviour can be reproduced with the full solution. In Fig. 2 this principle behaviour is demonstrated over a wide range of  $m_U$  and  $m_{\tilde{t}_R}$  for  $\tan\beta = 3$ . Nevertheless, for large (positive)  $m_U^2$  the used approximations become worse and corrections of order  $\mathcal{O}(m^2/T^2)$  are important. Then our approximations break down. However, this range is in any case physically disfavoured for a strong PT.

<sup>4</sup>Since eq. (3.11) depends through  $\mathbb{A}$  on  $v_w$  we solved it iteratively.

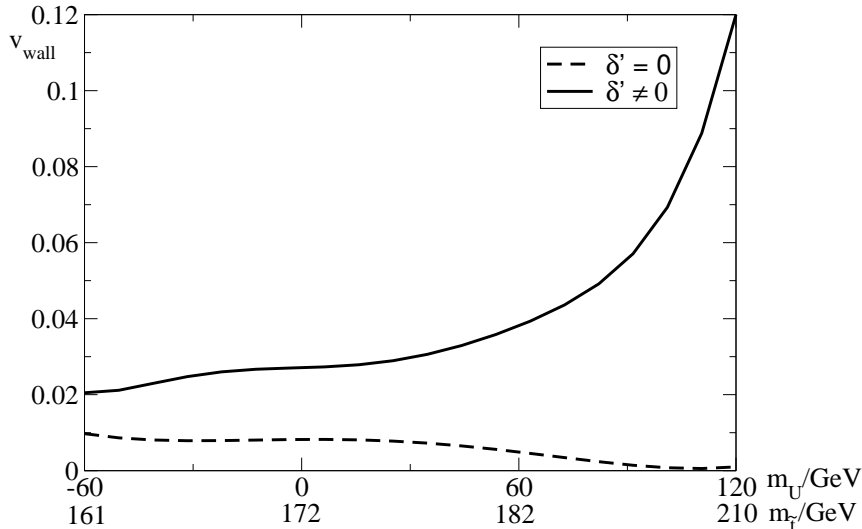


Figure 2: Wall velocity for increasing stop mass parameter  $m_U$ . At very large  $m_U$  (physically disfavoured) the stops decouple from the plasma leading to a large velocity while the first approximation  $\delta' = 0$  contrarily leads to decreasing  $v_W$ . The diagram is calculated for  $\tan\beta = 3$ ,  $A_t = \mu = 0$ , and  $m_A = 400\text{GeV}$ .

## 7 Conclusion and Discussion

The velocity of walls of expanding bubbles during the phase transition is an important ingredient for the calculation of the baryon asymmetry at the electroweak scale. In this paper we developed the utilities for the calculation of the wall velocity in extensions of the Standard Model and applied them to the MSSM. We generalized the method of [18] to include more than one Higgs field and arbitrarily many particles and applied it to the MSSM with a light right handed stop.

We estimated the effect of the stops on the wall velocity in the plasma of the simplest supersymmetric extension of the SM with all particles heavy or in equilibrium besides the light stop, the  $W$  bosons and the top quark. With our calculation we give lower bounds on the friction or viscosity coefficients of this plasma. There are two parts, one for the two CP even Higgs fields each. In the region of  $\tan\beta$  which is interesting for baryogenesis the velocity depends weakly on  $\tan\beta$  and we find values of  $\mathcal{O}(10^{-2})$ . We can answer the question of the title with *Yes*: stops slow down the bubble wall. We have not included effects of further out-of-equilibrium SUSY particles like charginos and neutralinos and gave only the leading order results. Gluinos may have considerable influence due to their multiple interactions. Also a more precise consideration of the mass of the outer

legs in the graphs presumably give an effect. We calculated in the massless limit, but especially for the stop this might be questionable. Moreover we neglected possible effects on the transition parameters due to a space dependent background temperature. A change in the nucleation temperature  $T_n$  and potentially large reheating might change the results. These effects may also affect a deviation of the bubble wall profile from the kink Ansatz, as discussed in [18].

The contribution of the stop in our WKB calculation appears to be at least of the same order of magnitude as the soft gauge boson contribution estimated in [28]. A further calculation using combined techniques including Bödeker's effective theory [29] were nevertheless useful.

Low wall velocities agree with the requirements of baryogenesis and enlarge the baryon asymmetry. Our results support the possibility that electroweak baryogenesis is a realistic scenario for baryon asymmetry of our Universe.

**Acknowledgements.** We thank D. Bödeker, A. Hebecker, S. J. Huber, B. Kastening, M. Laine, G. Moore and S. Weinstock for useful discussions. This work was partly supported by the TMR network *Finite Temperature Phase Transitions in Particle Physics*, EU contract no. FMRX-CT97-0122.

## References

- [1] K. Rummukainen, M. Tsypin, K. Kajantie, M. Laine, and M. Shaposhnikov, *Nucl. Phys.* **B532** (1998) 283–314, [hep-lat/9805013](#).
- [2] A. T. Davies, C. D. Froggatt, and R. G. Moorhouse, *Phys. Lett.* **B372** (1996) 88–94, [hep-ph/9603388](#).
- [3] S. J. Huber and M. G. Schmidt, *Eur. Phys. J.* **C10** (1999) 473–481, [hep-ph/9809506](#); S. J. Huber, in *Proceedings of SEWM 98, Copenhagen, 1998*, [hep-ph/9902325](#).
- [4] S. J. Huber and M. G. Schmidt, [hep-ph/0003122](#); S. J. Huber, PhD thesis, University of Heidelberg, Oct. 1999.
- [5] D. Bödeker, P. John, M. Laine, and M. G. Schmidt, *Nucl. Phys.* **B497** (1997) 387–414, [hep-ph/9612364](#).
- [6] J. R. Espinosa, M. Quirós, and F. Zwirner, *Phys. Lett.* **B307** (1993) 106–115, [hep-ph/9303317](#); J. R. Espinosa, *Nucl. Phys.* **B475** (1996)

- 273–292, [hep-ph/9604320](#); M. Carena, M. Quirós, and C. E. M. Wagner, *Nucl. Phys.* **B524** (1998) 3–22, [hep-ph/9710401](#); M. Losada, *Nucl. Phys.* **B537** (1999) 3–31, [hep-ph/9806519](#); M. Losada, *Nucl. Phys.* **B569** (2000) 125–157, [hep-ph/9905441](#); M. Laine and K. Rummukainen, *Nucl. Phys.* **B535** (1998) 423–457, [hep-lat/9804019](#); M. Laine and K. Rummukainen, *Phys. Rev. Lett.* **80** (1998) 5259–5262, [hep-ph/9804255](#).
- [7] J. M. Cline and G. D. Moore, *Phys. Rev. Lett.* **81** (1998) 3315–3318, [hep-ph/9806354](#); J. M. Cline, [hep-ph/9810267](#); J. M. Cline, Proc. of SEWM 98, Copenhagen, 1998, [hep-ph/9902328](#).
- [8] M. Pietroni, *Nucl. Phys.* **B402** (1993) 27–45, [hep-ph/9207227](#).
- [9] A. Pilaftsis and C. E. M. Wagner, *Nucl. Phys.* **B553** (1999) 3–42, [hep-ph/9902371](#).
- [10] D. Comelli, M. Pietroni, and A. Riotto, *Phys. Rev.* **D50** (1994) 7703–7714, [hep-ph/9406368](#).
- [11] K. Funakubo, S. Otsuki, and F. Toyoda, *Prog. Theor. Phys.* **102** (1999) 389–406, [hep-ph/9903276](#).
- [12] M. Laine and K. Rummukainen, *Nucl. Phys.* **B545** (1999) 141, [hep-ph/9811369](#).
- [13] P. John, PhD thesis, University of Heidelberg, 1999.
- [14] S. Huber, P. John, M. Laine, and M. G. Schmidt, *Phys. Lett.* **B475** (2000) 104–110, [hep-ph/9912278](#).
- [15] S. Davidson, T. Falk and M. Losada, *Phys. Lett.* **B463** (1999) 214 [hep-ph/9907365](#); F. Csikor, Z. Fodor, P. Hegedüs, A. Jakovác, S. D. Katz and A. Piróth, *Phys. Rev. Lett.* **85** (2000) 932–935, [hep-ph/0001087](#).
- [16] M. Carena, M. Quirós, A. Riotto, I. Vilja, and C. E. M. Wagner, *Nucl. Phys.* **B503** (1997) 387–404, [hep-ph/9702409](#).
- [17] M. Brhlik, G. J. Good and G. L. Kane, [hep-ph/9911243](#).
- [18] G. D. Moore and T. Prokopec, *Phys. Rev.* **D52** (1995) 7182–7204, [hep-ph/9506475](#); G. Moore and T. Prokopec, *Phys. Rev. Lett.* **75** (1995) 777–780, [hep-ph/9503296](#).

- [19] B.-H. Liu, L. McLerran, and N. Turok, *Phys. Rev.* **D46** (1992) 2668–2688; M. E. Carrington and J. I. Kapusta, *Phys. Rev.* **D47** (1993) 5304–5315; N. Turok, *Phys. Rev. Lett.* **68** (1992) 1803.
- [20] M. Dine, R. G. Leigh, P. Huet, A. Linde, and D. Linde, *Phys. Rev.* **D46** (1992) 550–571, [hep-ph/9203203](#); M. Dine, R. G. Leigh, P. Huet, A. Linde, and D. Linde, *Phys. Lett.* **B283** (1992) 319–325, [hep-ph/9203201](#); A. D. Linde, *Nucl. Phys.* **B216** (1983) 421.
- [21] O. Pantano, *Phys. Lett.* **B224** (1989) 195–200; P. Huet, K. Kajantie, R. G. Leigh, B.-H. Liu, and L. McLerran, *Phys. Rev.* **D48** (1993) 2477–2492, [hep-ph/9212224](#); J. C. Miller and O. Pantano, *Phys. Rev.* **D40** (1989) 1789–1797; J. C. Miller and O. Pantano, *Phys. Rev.* **D42** (1990) 3334–3343; M. Laine, *Phys. Rev.* **D49** (1994) 3847–3853, [hep-ph/9309242](#); J. Ignatius, K. Kajantie, H. Kurki-Suonio, and M. Laine, *Phys. Rev.* **D49** (1994) 3854–3868, [astro-ph/9309059](#); K. Enqvist, J. Ignatius, K. Kajantie, and K. Rummukainen, *Phys. Rev.* **D45** (1992) 3415–3428; K. Kajantie, *Phys. Lett.* **B285** (1992) 331–335; K. Kajantie, J. Potvin, and K. Rummukainen, NSF-ITP-92-55; K. Kajantie, L. Karkkainen, and K. Rummukainen, *Phys. Lett.* **B286** (1992) 125–130, [hep-lat/9204013](#); J.-W. Lee, K. Kim, C. H. Lee, and J. Ho Jang, [hep-ph/9909521](#).
- [22] J. M. Moreno, M. Quirós, and M. Seco, *Nucl. Phys.* **B526** (1998) 489–500, [hep-ph/9801272](#).
- [23] J. M. Cline and M. Joyce and K. Kainulainen, *Phys. Lett.* **B417** (1998), 79–86, [hep-ph/9708393](#).
- [24] P. John, *Phys. Lett.* **B452** (1999) 221–226, [hep-ph/9810499](#).
- [25] P. John, *Proceedings of SEWM 98, Copenhagen, 1998*, [hep-ph/9901326](#).
- [26] J. M. Cline, G. D. Moore, and G. Servant, *Phys. Rev.* **D60** (1999) 105035, [hep-ph/9902220](#).
- [27] K. Enqvist, A. Riotto, and I. Vilja, *Phys. Lett.* **B438** (1998) 273–280, [hep-ph/9710373](#).
- [28] G. Moore, *JHEP* **0003** (2000) 006, [hep-ph/0001274](#).
- [29] D. Bödeker, *Phys. Lett.* **B426** 351, [hep-ph/9801430](#).